Dynamically Shaped Magnetic Fields

Initial Animal Validation of a New Remote Electrophysiology Catheter Guidance and Control System

Eli S. Gang, MD; Bich Lien Nguyen, MD, PhD; Yehoshua Shachar, BS; Leslie Farkas, BS; Laszlo Farkas, MSEE; Bruce Marx, BSME; David Johnson, BSEE; Michael C. Fishbein, MD; Carlo Gaudio, MD; Steven J. Kim, MSEE

Background—To address some of the shortcomings of existing remote catheter navigation systems (RNS), a new magnetic RNS has been developed that provides real-time navigation of catheters within the beating heart. The initial experience using this novel RNS in animals is described.

Methods and Results—A real-time, high-speed, closed-loop, magnetic RNS system (Catheter Guidance Control and Imaging) comprises 8 electromagnets that create unique dynamically shaped ("lobed") magnetic fields around the subject's torso. The real-time reshaping of these magnetic fields produces the appropriate 3D motion or change in direction of a magnetized electrophysiology ablation catheter within the beating heart. The RNS is fully integrated with the Ensite-NavX 3D electroanatomic mapping system (St Jude Medical) and allows for both joystick and automated navigation. Conventional and remote navigational mapping of the left atrium were performed using a 4-mm-tip ablation catheter in 10 pigs. A multielectrode transseptal sheath allowed for additional motion compensation. Linear and circumferential radiofrequency lesion sets were performed; in a subset of cases, selective pulmonary vein isolation was also performed. Recording and fluoroscopic equipments were unaffected by the magnetic fields generated by Catheter Guidance Control and Imaging. Automated mode navigation was highly reproducible (96±8.4% of attempts), accurate (1.9±0.4 mm from target site), and rapid (11.6±3.5 seconds to reach targets). At postmortem examination, radiofrequency lesion depth was 78.5±12.1% of atrial wall thickness.

Conclusions—A new magnetic RNS using a dynamically shaped magnetic field concept can reproducibly and effectively reach target radiofrequency ablation points within the pig left atrium. Validation of the system in clinical settings is under way. **(*Circ Arrhythm Electrophysiol*. 2011;4:770-777.)**

Key Words: catheter ablation ■ atrial fibrillation ■ remote magnetic navigation ■ mapping ■ imaging ■ electrophysiology

In recent years, the application of remote navigational systems (RNS) to clinical electrophysiological catheter procedures has been the subject of intense technological and clinical research.[1–3] Although catheter ablation has long been an established therapeutic mode for troublesome cardiac arrhythmias, the development of RNS was spurred by the need to improve clinical outcomes in difficult cases, decrease the ionic radiation exposure to patients and staff, shorten the procedure times, and perhaps level the playing field among clinicians with variable experience and manual dexterity skills.

Clinical Perspective on p 777

One such RNS uses 2 large permanent magnets on each side of the patient's body to create a uniform magnetic field within the subject's chest (Stereotaxis, St Louis, MO).[2] Computer-guided mechanical movements of the magnets control magnetic field orientations. An ablation catheter with permanent magnets affixed to its tip is deflected such that the tip becomes aligned parallel to each new magnetic field orientation. Initial optimistic reports from several clinical sites[2,4] were tempered by disappointing outcomes in recent clinical trial of radiofrequency ablation comparing this RNS against conventional radiofrequency catheter ablation techniques in patients with 2 common rhythm disturbances, atrial flutter and atrial fibrillation (AF).[5–7] Difficulty in navigating to all regions of interest and inadequate lesion formation were postulated to be possible reasons for these results.

Received August 12, 2010; accepted May 26, 2011.

From the Electrophysiology Section, Division of Cardiology, Department of Medicine, Cedars-Sinai Medical Center, Los Angeles, CA (E.S.G., B.L.N.); Magnetecs Corp, Inglewood, CA (Y.S., Laszlo F., Leslie F., B.M., D.J.); the Department of Pathology and Laboratory Medicine, David Geffen School of Medicine at UCLA, Los Angeles, CA (M.C.F.); the Heart and Great Vessels Department, Umberto I Hospital, Sapienza University of Rome, Italy (B.L.N., C.G.); and St Jude Medical, St Paul, MN (S.J.K.).

The online-only Data Supplement is available at http://circep.ahajournals.org/lookup/suppl/doi:10.1161/CIRCEP.110.959692/DC1.

Correspondence to Eli S. Gang, MD, Cardiovascular Research Foundation, 414 N Camden Dr, Beverly Hills, CA 90210. E-mail gang@cvmg.com

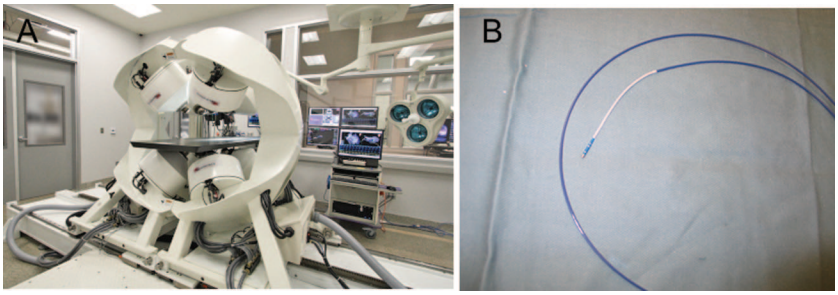

Figure 1. A, The Catheter Guidance Control and Imaging system used in these animal experiments is shown. Four of the 8 electromagnets can be seen. The fluoroscopy system is not shown. **B**, The quadripolar mapping ablation catheter. As described in the text, the distal (white) 10 cm is of a "floppy" construction.

In the current report, we describe our initial experience with a novel RNS, which uses new concepts in real-time magnetic navigation of a magnetically doped radiofrequency ablation catheter. The system described in this report provides precise, rapid, closed-loop control of this catheter within a fully integrated 3D electroanatomic mapping system. The initial experience, using this system in a series of anesthetized pigs undergoing an atrial mapping and ablation protocol, forms the body of this report.

Methods

Description of the System

The system used in these experiments (Catheter Guidance Control and Imaging, CGCI, Magnetecs, Los Angeles, CA) consists of 8 coil-core electromagnets arraigned semispherically, surrounding the subject's torso on a standard fluoroscopy table (Figure 1A). Unique construction of the electromagnets includes insertion of a ferrous ring at the end of a specially shaped magnetic pole face, both of which aid in the "focusing" of the magnetic field in the direction of the center of the subject's thorax. The coils are attached to a spherical steel structure that is uniquely designed so that the generated flux lines are magnetically conducted to return and close through an outer ferrous double C-arm structure via the center of the subject's torso. Thereby, the external parasitic magnetic stray fields are small. Additional magnetic shields are installed on the outer skin of the structure, preventing further stray magnetic fields, such that the measured electromagnetic radiation at a 12-inch distance from the center of the magnetic field is 20 Gauss, and at 24-inch a <5 Gauss field strength is measurable. When not in use, the electromagnets are completely disabled; hence there is no external residual magnetic field when the system is turned off. The electromagnets are cooled with 25 GPM glycol/water.

The 8-coil electromagnetic system generates a shaped ("lobed") dynamic magnetic field within the region of the subject's heart, contained within an approximately 6×6×6-inch cubic region with a maximal measured uniform field strength of 0.10 T. A newer "clinical" version of the CGCI generates up to 0.14-T field strength. By controlling the field magnitude, direction, and gradient, the generated magnetic fields can exert sufficient torque and force on a specially constructed magnetized catheter tip to cause it to be pushed/pulled and torqued (bent) within the cardiac chambers. The magnetic field gradient generated for force control of the catheter (translational or push-pull movement) is up to 0.7 T/m. Specifically, a real-time CGCI computer controller calculates the instantaneous current values for the 8 coils necessary to hold or move the catheter. The signal from the CGCI controller is amplified by 8 precision high-efficiency amplifiers; the currents and polarity in each of the coils is regulated in a manner that generates the uniquely shaped magnetic field ("magnetic lobe") that can be rapidly (ms) shaped to exert a desired torque or force on the magnetically doped catheter. Each coil is independently controlled, imparting 6 degrees of freedom for movement of the catheter tip. Accordingly, when a desired target is selected on the 3D representation of a cardiac chamber, the controller computer instantaneously computes the 8 coil currents necessary to generate the required dynamic field, which facilitates the movement of the catheter tip from its actual site to the desired site. These concepts are illustrated in Figure 2 A through 2F. In Figure 2A, a uniform magnetic field of a specific "shape" is illustrated which results in a horizontal catheter tip orientation. The strength of the magnetic field in different parts of the "lobe" is denoted by different colors, which are explained in the figure. In Figure 2B, the catheter tip is aligned parallel to the vector direction of the magnetic flux density, whose direction and magnitude are illustrated by arrows of varying sizes and colors. This change in vector direction of the magnetic field can be achieved in near–real-time speed. In Figure 2C, controller commanded changes in the current and polarity of the electromagnets have resulted in a shifting of the magnetic fields such that the catheter tip is now oriented in a 45° tip position. Figure 2D illustrates yet another rapid change in the torque field such that the catheter tip is aligned in a 90° configuration. In Figure 2E, a gradient magnetic "lobe" or field is illustrated, with a rapid and steady increase in magnetic field strength causing a translational "push-pull" movement of the catheter tip in the vertical direction. This is further illustrated in Figure 2F, wherein the arrows illustrate the magnetic density gradient in the direction of the catheter "pull." The magnitude of the tip "push-pull" can be controlled by the operator.

The subject's position on the fluoroscopy table is monitored with the use of optical fiducial patches, which provide dynamic compensation for gross body movements during the procedure. In these experiments, a motorized apparatus was taped to the groin of the subject, which enabled addition and removal of slack to the catheter, as commanded by the controller. The catheter slack control, however, is not an integral part of the catheter navigation, which, as noted above, relied on shaping of the magnetic field for torque and translational movement of the catheter tip.

Catheter Guidance Within the Heart

A 7F quadripolar radiofrequency ablation catheter with a 4-mm distal ablation electrode was fitted with a high-coercive magnetic pellet of neodymium based (Nd-Fe-B, N48) nano-crystalline material, and standard platinum electrode design and spacing. The magnet is entirely encased within a platinum shell, which protects the pellet from corrosion and fracture and ensures the biocompatibility of the device. The distal portion of the catheter, including the 4 electrodes and a thermistor, is approximately 20 mm in length. The distal most 10-cm of the catheter is of a "floppy" construction, thus allowing for its guidance and maneuverability using the external magnets described above (Figure 1B). The CGCI system includes integration with a digital fluoroscopic unit (Ziehm Imaging, Inc, Nuremberg, Germany), multichannel ECG recording and digital storage, intracardiac echocardiographic (ICE) display and storage, and full integration with a 3D electroanatomic mapping system, EnSite/NavX/Verismo (St Jude Medical, St Paul, MN).

CGCI Active Sheath

The CS catheter is used by NavX as a stable reference to locate the ablation catheter to eliminate respiratory movement of the heart and to transform a dynamic heart to a virtual static 3D representation.

The CS catheter, while providing a geometric and "field scaling" reference, did not always provide adequate motion compensation to a catheter that appeared to be moving out of phase with the CS reference, that is, the interatrial septal anchoring point of the

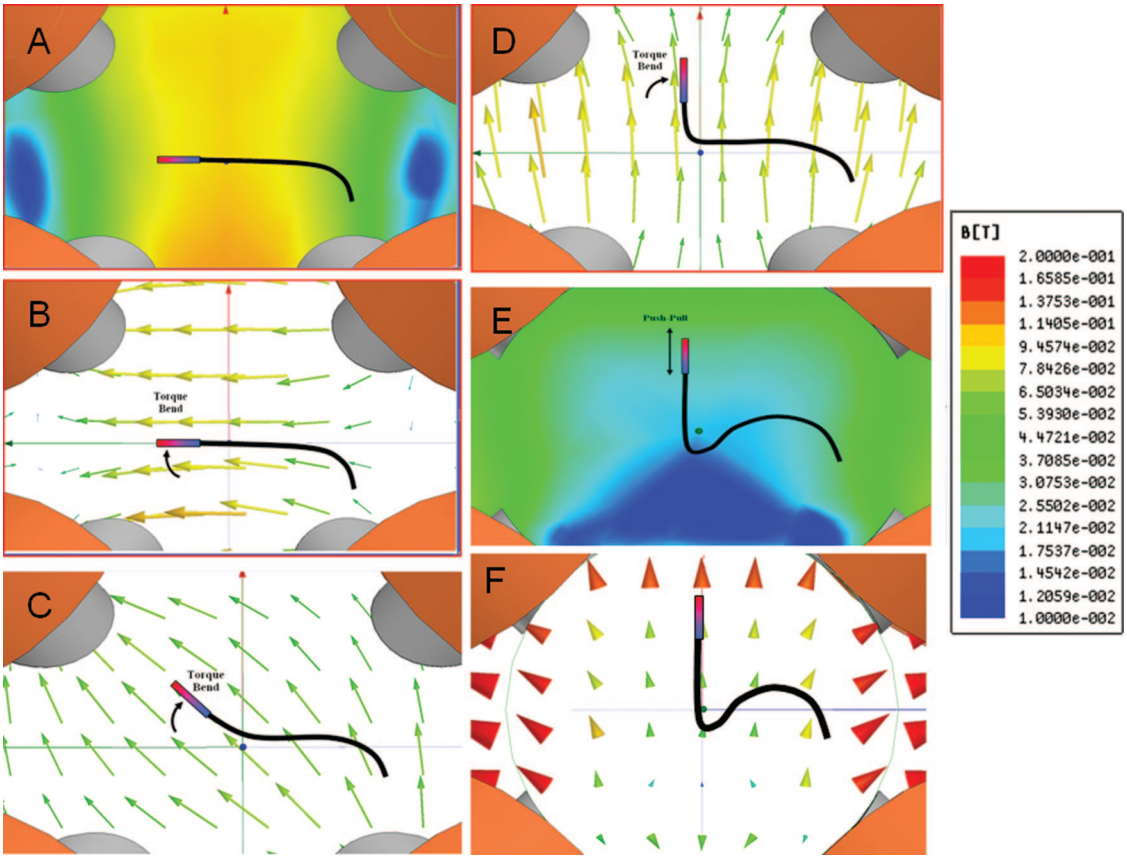

Figure 2. A, Cross-sectional view (4 of 8 magnets illustrated) of the uniform distribution of the magnetic field strength. In this example, the polarity of the 2 electromagnets on the left is such that the catheter tip is pointed in a horizontal direction. The color code in the adjacent table denotes magnetic field intensity, wherein the orange color is approximately 0.10 T. **B**, Vector magnitude and direction of the magnetic flux density is illustrated. The catheter is aligned parallel to the same vector direction shown in **A**. **C**, Near real-time change in the current and polarity of the electromagnets has resulted in a magnetic field that torques the catheter tip at a 45° angle. **D**, Torque field change has resulted in a 90° orientation of the catheter tip; **E** and **F**, The same format is used to show a magnetic field of increasing intensity, for example, a field gradient, resulting in a pulling of the catheter tip in the direction of increasing field strength (vertical upward movement, in these examples).

transseptal sheath appeared to have a motion separate and distinct from the motion of the mitral valve annulus and the CS catheter.

A CGCI "active transseptal sheath" was created by adding 5 standard platinum alloy electrodes placed along the distal end (5-mm interelectrode distance) of a transseptal sheath built to the SL-0 specifications (St Jude Medical) to remove the additional movement of the transseptal sheath and the ablation catheter from the NavX data stream that is provided to the CGCI controller.

Modes of Catheter Navigation

Two modes of catheter control are available to the operator of the CGCI system: (1) a Manual Magnetic mode ("man-in-the-loop") is a joystick-controlled mode that offers a nearly instantaneous responsive way to direct the catheter tip within a cardiac chamber, using the NavX closed-loop solution to delivering the catheter to an operator-designated site. For example, the operator can designate a series of points surrounding the ostium of a pulmonary vein (PV). (2) The CGCI logic routines will then plan a path to reach the targeted location, determine the optimal contact direction, and then guide the catheter tip until it makes a firm and continuous tissue contact. A tissue impedance measurement algorithm aids in determining the point of catheter-tissue contact, while tissue-contact sensing filters continue advancing the tip until continuous contact is reached over the entire cardiac cycle. Artificial intelligence (AI) routines are used in the following manner: If the catheter slips from a designated tissue location, the sensing system immediately alerts the magnetic field regulator and the tip is rapidly guided back into contact at the desired tissue location. As well, if an anatomic obstacle is detected during the catheter's travel to a designated point, the location is automatically marked and a new path is planned until tissue contact is achieved.

Catheter Tip Force Measurement

The force exerted by the catheter tip during application of a magnetic field were measured by an apparatus shown in Figure 3, which consisted of 2 nonmagnetic stands, one securing the sheath and the other holding a force gauge. Both were placed within the magnetic chamber of the CGCI. The force gauge was calibrated using 5 and 20 g precision calibration weights. The CGCI was controlled to generate a uniform magnetic field of 0.10 T, in a direction perpendicular to the flat plate of the force gauge. The perpendicular forces exerted by the catheter tip were measured at various lengths of catheter extruded from the sheath. The catheter bending point in these experiments was at the end of the sheath. The measured tip force at various extruded catheter lengths was compared with the predicted values calculated for a constant torque exerted by a constant magnetic field on the permanent magnetic tip with varying catheter lengths.

Animal Study Protocol

The animal experiments were performed on 15 farm pigs (S and S, San Diego, CA) weighting 35 to 70 kg, in accordance with Institutional Animal Research Committees, and National Institutes of Health guidelines. Each animal was premedicated with intramuscular acepromazine 0.25 mg/kg, and ketamine 20 mg/kg. Anesthesia was

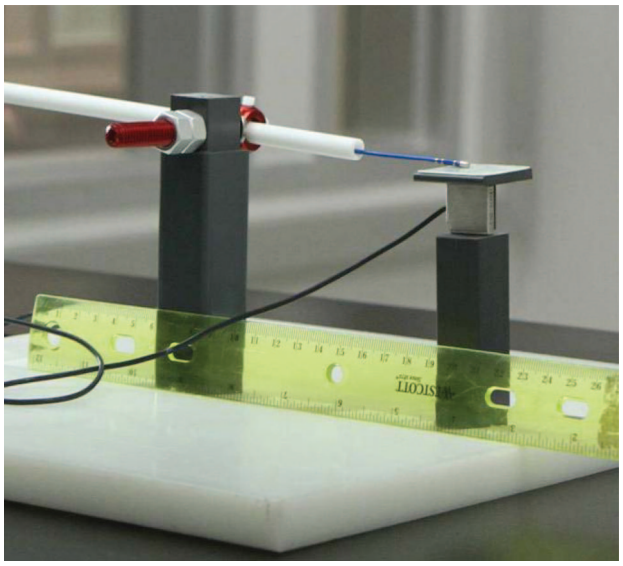

Figure 3. Experimental setup for measuring the catheter tip force. The magnetic tip of the catheter rests on a force gauge platform. A magnetic field with an intensity of 0.10 T is generated that points in a downward, perpendicular direction. Tip force was measured at various catheter lengths.

induced with intravenous thiopental 5 to 8 mg/kg, followed by endotracheal intubation and ventilation. Inhalational general anesthesia was maintained with 1% to 2% isoflurane. Bilateral femoral and right internal jugular venous endovascular access sheaths were placed the usual sterile fashion. A 7F decapolar CS catheter (CSL, St Jude Medical) was manually positioned in the body of the CS under fluoroscopic guidance. The transseptal puncture was performed using a standard approach from the right femoral vein, under fluoroscopic and ICE ultrasound (ACUSON AcuNav, Siemens, Erlangen, Germany) guidance using a Brockenborough (BRK series, St Jude Medical) needle technique delivered through the SL-1 sheath (St Jude Medical). Unfractionated heparin was administered intravenously, once access to the left atrium (LA) was achieved, to maintain the activated clotting time >250 seconds. LA mapping and creation of a 3D NavX map of the LA and associated PVs was initially performed manually using a 4-mm conventional ablation catheter (Safire, St Jude Medical) and conventional variable 15- to 25-mm circular mapping catheter (Spiral, St Jude Medical). The standard transseptal sheath was then exchanged over the wire with the proprietary modified electrode transseptal sheath. Mapping of the LA was repeated, using the CGCI Manual Magnetic mode (joystick activated), and the 2 maps compared. In a subset of pigs, a preprocedure 64-slice contrast-enhanced computed tomography (CT) scan (GE, Waukesha, WI) of the LA and PVs was obtained under general anesthesia. The CT image of the LA was fused into the NavX map using Verismo software. Once the 3D geometry of the LA chamber was completed, predefined sites on the 3D map were targeted in the following manner. To demonstrate reproducible agility and accuracy of the navigation system, a set of linear and circumferential discrete target points were created on the NavX map of the left atrium. The linear target sets were usually on the roof of the LA or at the mitral valve-left PV region, whereas the circular sets were at the orifice of the appendage or of one of the PVs, when of sufficient size. Both the manual as well as the automated magnetic modes were used to reach the target sets. In the automated magnetic mode, a minimum of 5 attempts was required to reach each designated target point, and quantitative measurements of accuracy, repeatability, time to reach target, stability, and reproducibility at each site, were obtained and recorded. CGCI provided an online readout of distance from target point. The catheter was returned to the middle of the chamber after each attempt. Reaching a target was defined as being within <2 mm from the designated NavX site, and the distance from target was continuously displayed. To validate the observation that specific target points had been reached using the automated magnetic navigation mode, on reaching the target for the first time, radiofrequency energy was delivered for approximately 30 to 40 seconds, at 30 to 40 W, with a target temperature of 55°C. Although this was not an end point of the protocol, in a subset of animals, PV isolation was also attempted. Intracardiac electrograms (EGMs) within the targeted PV were measured before and after creation of a circumferential radiofrequency lesion set, and vein isolation was confirmed by demonstrating exit block while pacing within the targeted PV as well as entrance block by loss of EGM signal within the targeted vein.

Pathological Gross Inspection of Organs, Sample Processing, and Histological Analyses

The animals were euthanized, and the heart, lungs, esophagus, kidneys, liver, and spleen were immediately removed and fixed in 10% formalin for detailed gross and histological tissue analyses by a blinded pathologist at UCLA (M.C.F.) to identify any cardiac or extracardiac pathology. Navigational cardiac target sites were examined for evidence of gross tissue trauma. The atrial sites with radiofrequency lesions were sampled, processed for histological analysis, stained with hematoxylin and eosin and trichrome, and characterized measuring transmurality (percentage of the tissue transmural thickness), contiguity (mm overlap or distance between 2 lesions), width (mm), depth (mm), and location (mm of distance between the site on NavX/fluoroscopy, and the site on histology).

Statistical Analysis

Continuous variables are expressed as mean±SD, and categorical variables are expressed as percentages.

Results

Fifteen pigs were used in this study. Five animals were excluded from analysis: The first 3 pigs were used to gain confidence in navigating the magnetic catheter in the pig's cardiac chambers; 1 pig died of an arrhythmic event before initiation of remote navigation; 1 pig had a subclinical perforation of the LA wall caused by a traumatic endothelial sharp-edge tear and tissue disruption caused by the transseptal puncture and subsequent radiofrequency application at the same site. The radiofrequency thermal lesion was seen to include 25% of the outer adventitial wall of an adjacent pulmonary artery. Thus, the LA remote navigation and ablation protocol was performed in the remaining 10 pigs.

Fidelity of the ECG, Intracardiac Recording, and ICE During Application of Magnetic Fields

Standard surface ECGs and intracardiac EGMs were recorded in the presence and absence of a 0.10 T (maximum) magnetic field. Distal-pair, bipolar intracardiac EGM recordings were made with a magnetic 4-mm-tip catheter at the LA wall, and a right atrial His-bundle EGM also obtained in the first experiment. No qualitative differences in the fidelity of the recorded signals were noted in the presence of magnetic fields. Stimulation pacing thresholds at LA sites were obtained during manipulation of a conventional electrode catheter as well as during remote magnetic navigation of magnetic catheter. Pacing thresholds below 3 mA were achieved with both methods. ICE images were continuously available during magnetic catheter navigation. No degradation of the ICE images was seen during application of the variable magnetic fields.

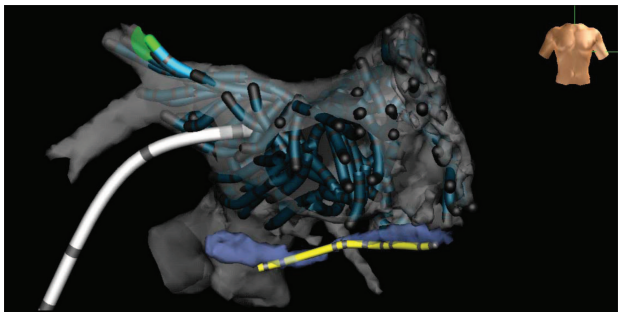

Figure 4. Sites of travel of the magnetic catheter within the CT generated left atrial chamber. Each site had been stored in NavX and reproduced with a catheter tip image. A transseptal sheath (white), Catheter Guidance Control and Imaging catheter in a pulmonary vein (green), and a CS electrode catheter (yellow) are also seen.

Catheter Tip Force Measurement

The perpendicular forces exerted by the catheter tip on the force gauge plate were proportional to the length of the catheter extruded from the sheath. This length, including the distal 20-mm casing, ranged from 30 to 70 mm. The measured force ranged from 5 g at 70-mm catheter length, to 23 g at 30-mm catheter length. Catheter tip forces measured at 45° and at 90° were of similar magnitude (5 to 27 g) and dependent on length of extruded catheter (graph available in the online-only Data Supplement).

Remote Electroanatomic Mapping of the LA and PVs

Creation of an LA-PV 3D (NavX) map was performed in the manual magnetic mode in all animals. Despite the relatively small size of the porcine atria and the typical short distance between the transseptal puncture and the posterior LA wall, it was possible to enter and navigate into PVs in all 10 animals. The magnetic catheter was successfully advanced into a total of 37 PVs. A representative experiment from a single animal is shown in Figure 4, demonstrating the sites of navigation of the magnetic catheter within the LA and the PVs, and the tubular renderings of the PVs. Remote magnetic mapping time was 30.6±13.5 minutes, using CGCI manual magnetic mode.

Remote LA and PV-LA Junction Navigation and Ablation

As noted, radiofrequency ablation was used for "tagging" the anatomic sites to which the magnetic catheter was navigated. Using the view-synchronized 3D CT scan and NavX map, the CGCI ablation catheter was navigated in the manual and automatic modes, but the automatic mode was used to perform linear and circumferential radiofrequency ablation lesions during sinus rhythm. The overall number of radiofrequency target sites was 29.7±7.1 per animal. A series of linear atrial radiofrequency lesions was deployed (30 to 40 W, 55°C temperature limited, 30 to 40 seconds) at the LA

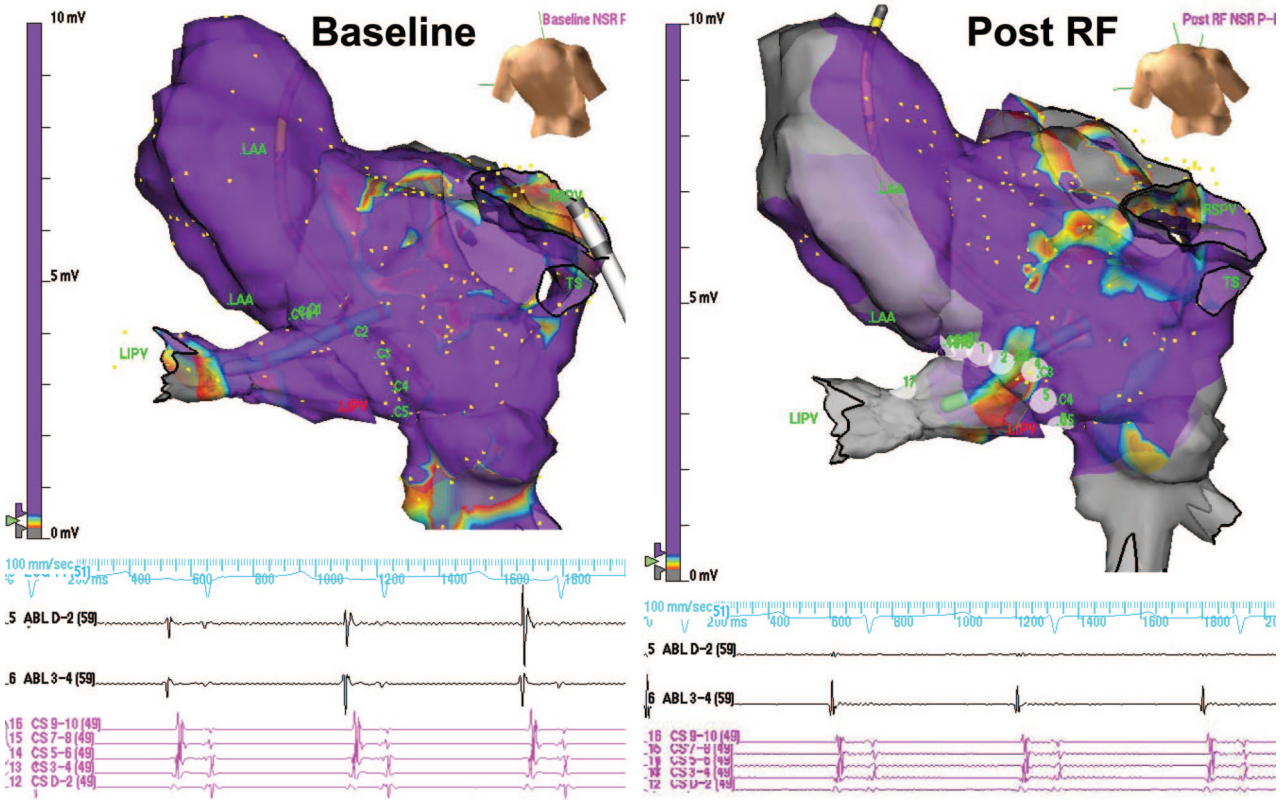

Figure 5. Pulmonary vein (PV) isolation. **Baseline**, The catheter had been navigated to each of the predesignated circumferential ablation sites (marked C in the first panel) at the ostium of the PV. Discreet atrial and small ventricular signals are seen. **Post RF**, Second panel shows loss of voltage in the target PV as well as absence of electric activity in the distal 2 electrodes, with the catheter placed just beyond the ostial circumferential lesion set.

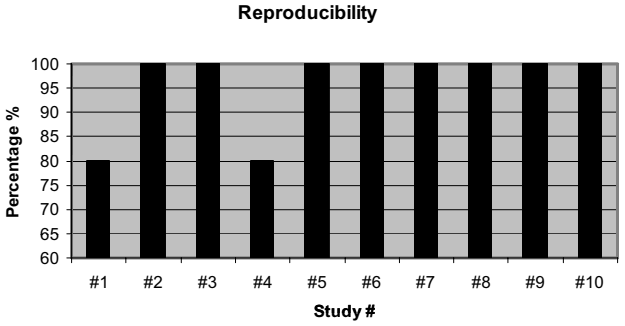

Figure 6. Graph illustrating reproducibility of returning to specific sites in automated navigation mode.

"roof," connecting a superior PV and the LA appendage (LAA), or at the mitral isthmus, connecting the left lower PV to the lateral mitral annulus. Between each radiofrequency application, the catheter was navigated along a linear trajectory across the endocardial surface. The lines were composed of 7.2±3.2 linear target points.

Circumferential radiofrequency lesion sets were created (30 to 40 W, 50° to 55°C, ≈40 seconds) around the base of the LAA or the PV ostia. The circles were composed of 16.1±4 targets sites. After each application of radiofrequency energy, the catheter was withdrawn to the center of the LA chamber, and the targeting process was repeated. Target site acquisition was defined as having reached within ≤2.0 mm of the selected NavX target site, a distance displayed on the CGCI console. In 8 of 10 pigs, a total of 11 PVs were targeted for radiofrequency ablation, that is, circumferential lesion sets were placed around the ostium of each vein: 6 right PVs and 5 left PVs. In the last 2 pigs, actual verification of PV isolation was confirmed by voltage mapping and pacing maneuvers (entrance and exit conduction block in 3 of 3 veins thus tested (Figure 5). Automatic mode catheter navigation efficiency was quantified for target site acquisition in the linear and circumferential lesion sets. This analysis was not applied to the PV isolation lesion sets because these were not performed in each animal. In each experiment, the following data were tabulated:

(1) Repeatability: Defined as (successful-failed)/successful target acquisition=91±8.3%.

(2) Reproducibility: Defined as ability to acquire the same stable point 5 consecutive times=96±8.4% (Figure 6).

(3) Accuracy: Defined as final distance from the fixed NavX map target point=1.9±0.4 mm.

(4) Time to reach target: Defined as time from initiation of catheter travel from a midchamber departure point to the target designated point, including avoidance of anatomic barriers=11.6±3.5 seconds.

Postmortem Studies

Necropsy revealed that the linear and circumferential radiofrequency lesions were visible on the epicardial surface of the heart (Figure 7). Postmortem pathological examination revealed no cardiac perforations. No damage to adjacent or remote organs was seen. radiofrequency lesions were uniformly situated around the PV ostia, around the LAA base, roof, and mitral isthmus. Overall radiofrequency lesion depth was 78.5±12.1% of entire LA wall thickness. The majority of the radiofrequency lesions were transmural (Figure 8). Nontransmurality was usually seen at LAA trabeculated tissue, where the tissue thickness exceeded the thickness found at the PV-LA junction or at the ostia of the PVs.

Discussion

We describe a new RNS that uses an external array of electromagnets to generate rapidly changing force fields that have the capacity to move a magnetically tipped catheter within a cardiac chamber at real-time speed and efficiency. We also demonstrate the feasibility of this new system in an in vivo set of experiments, in which extensive navigation within the LA of anesthetized pigs was undertaken to simulate the catheter movements needed to perform a clinical radiofrequency ablation case within the confines of the beating heart.

The magnetic RNS described in this report is novel in the following ways:

(1) In contrast to an existing magnetic RNS, the system described herein has no moving components responsible for changes in the orientation of a magnetic field. Rather, the magnetic field is continuously and rapidly shaped and reshaped according to the navigational needs of the user, yielding a uniform torque vector field, which exerts a bending or rotating effect on the permanent magnetic tip of the catheter in 3D space, or a magnetic field gradient that provides axial push-pull movement The ability to vary the

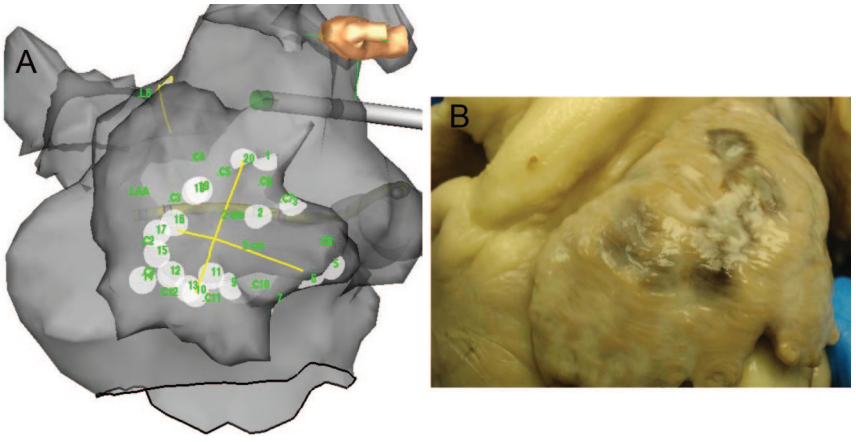

Figure 7. Epicardial and 3D map location of circumferential radiofrequency lesion set at the LAA. There was excellent correlation between NavX estimation of diameter of circle (2 cm) (**A**) and epicardial evidence of transmural lesions at most ablation sites (**B**).

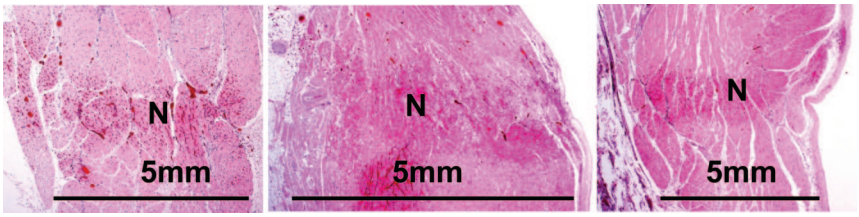

Figure 8. Histological evidence of transmural necrosis (N) induced by radiofrequency thermal injury. Necrotic regions are stained red.

intensity of the torque and force fields also differentiates the CGCI from the existing magnetic RNS.

(2) The system design minimizes parasitic external magnetic forces, which may allow undisturbed use of other electronic medical equipment and eliminates the need for additional shielding of the procedure room.

(3) When operating in the automatic mode, the CGCI RNS is a true closed-loop servo system that also has the ability to keep the catheter tip on a desired anatomic target by continuously adjusting the direction and intensity of the magnetic fields such that the magnetic tip of the catheter can be repeatedly returned to a target anatomic site.

The maximal generated magnetic field forces generated by the CGCI system exceed the published field forces of the existing magnetic RNS[2,5–7] (up to 0.10 T and 0.15 T, in the "preclinical" and "clinical" units, respectively, versus the reported 0.08 T for the Niobe RNS system). Using another magnetic RNS, 2 recent AF[5,6] ablation studies showed PVI in only 8% of the patients when using the Niobe II magnetic RNS with a nonirrigated radiofrequency ablation catheter, and PVI in 95% of the cases, but with caval-tricuspid block achieved in only 50% of patients with an irrigated-tip magnetic catheter. Fluoroscopy and procedure times were significantly longer with the magnetic RNS than with the conventional approach.[6] In a study of "typical "atrial flutter ablation, RNS-guided caval-tricuspid ablation resulted in a significantly lower success rate and a larger number of radiofrequency energy applications.[7] The authors of these studies postulated that the relatively poor outcomes were due to difficulty in navigating the magnetic catheter to certain regions of the atria and weaker catheter endocardial contact forces exerted by the RNS-assisted magnetic catheter when compared with those exerted by manually controlled ablation catheters. This may explain the longer fluoroscopy[6] and total radiofrequency times,[6,7] longer procedure times,[6,7] and lower caval-tricuspid block success rates[6,7] as probably being due to inadequate lesion depth formation by the RNS system.

In our study, we used a nonirrigated catheter, lower-energy settings and shorter radiofrequency application times because the study was intended to show the agility and maneuverability of the CGCI system rather than to achieve large lesions. Nonetheless, our postmortem results showed a mean lesion depth of 78.5±12% of the LA wall thickness, with the majority of the radiofrequency lesions being transmural. PV ostial isolation was achieved in some pigs in this study, but was, again, not a study end point and not attempted in each experiment.

Recent ex vivo experiments have confirmed the hypothesis that catheter contact force is a major determinant of radiofrequency lesion size.[8] In superfused dog thigh muscle preparations, reasonable lesion size and depth as well as minimal incidence of thrombus formation and steam pops were seen at irrigated catheter contact forces between 10 and 30 g, which agrees with the range of forces measured with the catheter and CGCI system described in this report. Based on the results presented in this study, the novel system capabilities of the CGCI may allow for enhanced catheter navigation, target acquisition, as well as enhanced adherence to the ablation target site in the clinical electrophysiology laboratory and thereby facilitate the fulfillment of the promise of robotic catheter navigational systems in the treatment of cardiac arrhythmias.

Potential System and Study Limitations

The magnetic RNS system described in this study has some potential limitations. Similar to any RNS, the user is removed from the patient's bedside; monitoring of patient's clinical status must be ensured. Because the CGCI system is completely integrated with a 3D mapping system (NavX), the accuracy of target acquisition is limited to the accuracy of the mapping system. The catheter used in these experiments was a nonirrigated prototype; clinical work with irrigated and nonirrigated versions remains to be done. Most of the experiments were performed by navigating the magnetic catheter within the confines of the normal porcine LA. The limitations of working within the pig's heart are well described.[9] The typical porcine LA receives only 2 main PV ostia and an azygous vein, in contrast to the typical 4 PVs that drain into the human LA. The LAA comprises a large portion of the porcine LA volume, in contrast to the typical human LA. The body of the LA (PV ostia and LAA excluded) tends to be rather small in the pig, averaging approximately 20 mm in diameter in our subjects. Extrapolation of results from this study to normal and enlarged human left atria remains to be proven. For example, efficacy of radiofrequency energy application to traditional "difficult" anatomic sites such as the RIPV remains to be demonstrated in the human LA. Also, the utility of this system was not systematically tested in other cardiac chambers. Finally, PV isolation was not performed in each pig, and the completeness of conduction block was not tested for linear lesion sets because neither was an aim of the study.

Conclusions

Initial feasibility studies of a new remote navigational system are described and provide encouraging results. Clinical trials are currently under way to validate these initial observations.

Acknowledgments

Dr Nguyen is a recipient of the PhD Fellowship in "Tecnologie Biomediche in Medicina Clinica" at Sapienza University of Rome, Italy.

Sources of Funding

This study was supported by the Chun Hwang Fellowship for Cardiac Arrhythmia honoring Dr Asher Kimchi, Taylor Family Foundation, Electrophysiology Section, Division of Cardiology, Department of Medicine, Cedars-Sinai Medical Center, Los Angeles (Dr Nguyen), and by Magnetecs Corp.

Disclosures

Dr Gang and Yehoshua Shachar have equity interest in Magnetecs Corp.

References

1. Faddis MN, Blume W, Finney J, Hall A, Rauch J, Sell J, Bae KT, Talcott M, Lindsay B. Novel, magnetically guided catheter for endocardial mapping and radiofrequency catheter ablation. *Circulation*. 2002;106: 2980–2985.
2. Pappone C, Vicedomini G, Manguso F, Gugliotta F, Mazzone P, Gulletta S, Sora N, Sala S, Marzi A, Augello G, Livolsi L, Santagostino A, Santinelli V. Robotic magnetic navigation for atrial fibrillation ablation. *J Am Coll Cardiol*. 2006;47:1390–1400.
3. Reddy VY, Neuzil P, Malchano ZJ, Vijaykumar R, Cury R, Abbara S, Weichet J, McPherson CD, Ruskin JN. View-synchronized robotic image-guided therapy for atrial fibrillation ablation: experimental validation and clinical feasibility. *Circulation*. 2007;115:2705–2714.
4. Ernst S, Ouyang F, Linder C, Hertting K, Stahl F, Chun J, Hachiya H, Bansch D, Antz M, Kuck KH. Initial experience with remote catheter ablation using a novel magnetic navigation system. *Circulation*. 2004;109: 1472–1475.
5. DiBiase L, Fahmy TS, Patel D, Bai R, Civello K, Wazni OM, Kanj M, Elayi CS, Ching CK, Khan M, Popova L, Schweikert RA, Cummings JE, Burkhardt JD, Martin DO, Bhargava M, Dresing T, Saliba W, Arruda M, Natale A. Remote magnetic navigation: human experience in pulmonary vein ablation. *J Am Coll Cardiol*. 2007;50:868–874.
6. Miyazaki S, Shah A, Xhaet O, Derval N, Matsuo S, Wright M, Nault I, Forclaz A, Jadidi AS, Knecht S, Rivard L, Liu X, Linton N, Sacher F, Hocini M, Jais P, Haissaguerre M. Remote magnetic navigation with irrigated tip catheter for ablation of paroxysmal atrial fibrillation. *Circ Arrhythm Electrophysiol.* 2010;3:585–589.
7. Vollmann, Luthje L, Seegers J, Hasenfuss G, Zabel M. Remote magnetic catheter navigation for cavotricuspid isthmus ablation in patients with common-type atrial flutter. *Circ Arrhythm Electrophysiol*. 2009;2: 603–610.
8. Yokoyama K, Nakagawa H, Shah DC, Lambert H, Leo G, Aeby N, Ikeda A, Pitha JV, Sharma T, Lazz R, Jackman WM. Novel contact force sensor incorporated ion irrigated radiofrequency ablation catheter predicts lesion size and incidence of steam pop and thrombus. *Circ Arrhythm Electrophysiol*. 2008;1:354–362.
9. Crick SJ, Sheppard MN, Ho SY, Gebstein L, Anderson RH. Anatomy of the pig heart: comparisons with normal human cardiac structure. *J Anat*. 1998;193:105–119.

CLINICAL PERSPECTIVE

Catheter ablation has become a mainstay in the treatment of cardiac arrhythmias. Robotic, or remote machine-guided navigation of electrode catheters, holds the promise, for facilitating ablation procedures and reducing radiation exposure. This report describes our initial experience in validating a new, remote magnetic catheter navigation system in the animal laboratory. The system has 8 electromagnets surrounding the torso of the experimental subject, which are able to producing rapidly changing magnetic fields to guide magnetic catheters to the desired target region. Automated controls keep the catheter at its designated anatomic target and a closed-loop guiding system provides rapid course correction as the catheter tip is automatically guided toward anatomic targets on a 3D mapping system. Our initial animal experiments suggest that this is a safe and effective means of navigating an ablation catheter within the confines of the porcine left atrium. Moreover, no specific magnetic shielding of the room is necessary with this system. Clinical trials are under way to assess the utility of this system in the clinical electrophysiology laboratory.

Dynamically Shaped Magnetic Fields: Initial Animal Validation of a New Remote Electrophysiology Catheter Guidance and Control System

Eli S. Gang, Bich Lien Nguyen, Yehoshua Shachar, Leslie Farkas, Laszlo Farkas, Bruce Marx, David Johnson, Michael C. Fishbein, Carlo Gaudio and Steven J. Kim

Circ Arrhythm Electrophysiol. 2011;4:770-777; originally published online June 20, 2011;
doi: 10.1161/CIRCEP.110.959692
Circulation: Arrhythmia and Electrophysiology is published by the American Heart Association, 7272 Greenville Avenue, Dallas, TX 75231

Print ISSN: 1941-3149. Online ISSN: 1941-3084

Supplemental Material

1. Description of fluoroscopy unit: The fluoroscopy unit is a single-plane fluoroscopy unit which has been integrated into the CGCI system in the following ways: (a) The magnetic fields do not distort the fluoro image (b) the user can command the fluoroscopy angle from the workstation, with up to approximately 45° LAO and RAO oblique projections (d) the new "clinical" systems have up to 20 kVA capability, which allows for enhanced fluoroscopic image quality.
2. Optical fiducial patches: CGCI used in these experiments incorporated the Boulder Innovations Fiducial Tracking System, which uses a multi-LED sensor to optically track the patient position and orientation in six-degrees of freedom. The sensor is attached to the patient's chest in close proximity to the center of the EnSite coordinate system. After the fiducial system is activated, any shift in the patient's position and orientation causes a re-alignment between the patient's local coordinate system and the CGCI's global coordinate system. This allows the CGCI to maintain data integrity and system controllability throughout the procedure.
3. 'Active transseptal sheath' concept: Early in our work on the first 2 pilot pig experiments, we noticed that frequently the motion of the interatrial septum is out of phase with the motion of the coronary sinus. While NavX compensates for the motion of the CS reference catheter, we noticed that the septal sheath movement, with the distal end of the sheath serving as the anchor point for the EP catheter, introduced error into our magnetic mapping and to the stability of our regulator. We initially modified a standard SL1 sheath by adding several electrodes to it distal end; we subsequently modified a standard Agilis sheath (St. Jude Medical) in the same manner. This sheath is now being sold commercially by St Jude under the name of Agilis ES (in Europe). These electrodes serve as a dynamic reference for motion compensation. As NavX now recognizes the position and vector of the distal end of the sheath, software was written that subtracts this motion from the catheter's position at any given time (similar to the respiration compensation used by NavX). The catheter motion is thus seen only in reference to a 'static' septal wall of the Ensite map, thus giving our regulator better control of the catheter and giving the user a more accurate view of the catheter's location with respect to the static Ensite map. An interesting byproduct of this development was our ability to "shadow" the position of the Agilis sheath within the foramen ovale after performing the transseptal puncture. On those occasions that the left atrial catheter slipped back into the right atrium, joystick magnetic navigation of the catheter back to the left atrium was rapidly performed.
4. Tissue impedance measurement: At the discretion of the user, catheter tip tissue contact can be registered by viewing a continuous, on-line display of a complex impedance measurement (so-called 'electrical coupling index', or ECI) which has been developed by St Jude Medical. Initial clinical experience with this algorithm has recently been published (JCE, 2009, 20:1366-1373).
5. Torque and gradient magnetic fields: The 8 electromagnets are designed such that they can almost instantaneously (within ~200 msec) create a dynamic new magnetic field which can cause the tip of a magnetic EP catheter to 'torque', or bend, in the desired direction. They can do this by rapidly changing the polarity and/or intensity of the current within any combination of the 8 coils. In addition, a magnetic field gradient can be created in any direction, such that a

continuous increase in magnetic field strength in a certain direction will cause the catheter tip to be pulled in that direction. Within the confines of small chambers such as the left atrium of the pig, the CGCI was mostly a "torque system," i.e., once the catheter was across the septum and some slack provided, most of the maneuvering was done by bending the catheter in various directions and automatically adding or withdrawing slack. It is likely that in larger human chambers, such as the ventricles, the translational force generated by changing the force field will become more important. With the above in mind, the tip force measurement shown in Figure 3 represents maximal torque forces applied with the catheter tangential to the measuring platform. The 'Force vs. Catheter Length' graph shown below illustrates the calculated and actual measured relationship between the length of catheter extruded out of the guiding sheath (expressed in mm, not including the distal 20mm electrode-magnet assembly) and catheter tip force.

6. Maximal push-pull force: with the amount of magnetic material contained within the EP catheter used in these experiments and with the size of the electromagnets used in the described system, the push-pull force did not add more than ~5 gm of force. The newer 'clinical' design incorporates stronger electromagnets which are likely to provide additional push-pull force.